Research Article

The assessment of soil depth sensitivity to dynamic behavior of the Euler-Bernoulli beam under accelerated moving load

Amin Ghannadiasl [a],* (iD), Hasan Rezaei Dolagh [a] (iD)

[a] *Department of Civil Engineering, University of Mohaghegh Ardabili, 56199-11367 Ardabil, Iran*

ABSTRACT

Dynamic behavior is one of the most crucial characters in the railways structures. One of the items which leads to precise identification of the dynamic behavior of railways is the soil depth beneath them. In this paper, an Euler-Bernoulli beam on a finite depth foundation under accelerated moving load is presented. The dynamic equilibrium in the vertical direction is only regarded in accordance with the factor of finite beams. In this study, the dynamic equilibrium of the soil in the vertical direction and the sensitivity of soil depth are considered. The governing equations are simulated by using Fourier transform method. Eventually, by considering the sequences of shear waves, and different kinds of damping, displacement of the beam is obtained for the various acceleration, times and soil depth. As a result, it is shown that, higher acceleration is not dramatically effective on the beam displacement. Also, foundation inertia causes a significant reduction in critical velocity and can augment the beam response.

ARTICLE INFO

1. Introduction

Dynamic behavior of structures under accelerated moving loads is an important field in engineering. Hence, a lot of researches are done in this case. Problems that are occurred by these kinds of loads cannot be neglected in the structures behavior. For instance, the displacement of the beam by considering speed and acceleration is effected by train force on the railways.

Several studies have been derived in the dynamic behavior of the beam under various types of loads. The initial research on the elastic foundation is performed by Timoshenko (1926). His work relates to the response of the railway under the constant speed of moving load. Kenney (1954) obtained a steady-state solution and showed that the critical velocity is really effective on the deformation of the beam. The frequency of the beam vibrations by using of finite element method was derived by Györgyi (1981). Li (2000) presented a simple and unified approach for analyzing the free vibration of the generally supported Euler-Bernoulli beam. The linear association of the Fourier series and an auxiliary polynomial

function are used to specify the displacement of the desired beam. Hillal and Zibdeh (2000) recommended the vibration of the Euler-Bernoulli beam under moving load as a closed form solution. Also, an approach for extracting the dynamic behavior of damped Euler-Bernoulli beam excited by concentrated and distributed forces is provided by Abu-Hillal (2003). Kargarnovin and Younesian (2004) investigated the dynamic response of Timoshenko beam subjected to harmonic moving load with infinite length in the viscoelastic Pasternak foundation. Ying et al. (2008) studied the rough solutions for shear bending behavior and free vibration on the Winkler-Pasternak elastic foundation. Mehri et al. (2009) derived the dynamic behavior of the Euler-Bernoulli beam excited by moving load by using the Green function. Also, spectral analysis of the beam under the influence of load is recommended by Gladyzs and Sniady (2009). The desired beam is contemplated orthotropic at any point, whereas the properties of different materials in the thickness of beam are exponential. In addition, by using differential transform method the vibration of the Timoshenko and Euler-Bernoulli beam on elastic soil is predicted by

Balkaya et al. (2009). In this suggested method, accurate solutions without the serious analysis necessity are attained. Motaghian et al. (2011) investigated the problem of free vibration of the Euler-Bernoulli beam on the elastic foundation. Also, the nonlinear vibration of the Euler-Bernoulli beam with fixed ends under the influence of axial loads is derived by Barari et al. (2011), subjected to a bending load excitation while damping effect has been taken into account. A new analytical solution to predict the free lateral vibration of a Timoshenko beam with different kinds of boundary conditions is employed by Bazehhour et al. (2014). Also, the influence of the axial load on the natural frequencies is examined. Simultaneously, Prokić et al. (2014), illustrated a numerical approach to clarify the free vibration of Timoshenko beams with optional boundary conditions. The numerical approach is fundamentally attributed to numerical integration instead of the numerical differentiation. A proficient analytical approach to analyze the vibration of the Euler-Bernoulli beam on Winkler foundation is presented by Yayli et al. (2014). To attain the free vibration response of the beam on Winkler foundation, the Stoke's transformation with Fourier sine series is utilized. The dynamic response of the railway track structure subjected to moving load on visco-elastic foundation is derived by Mohammadzadeh and Mosayebi (2015). An analytical method and a combined finite element for predicting the vibration of a crane system subjected by suspended moving body is provided by Zrnić et al. (2015). Bian et al. (2016) presented the dynamic response of the railway under constant and accelerated moving loads with various velocities. For this purpose, the railways were modeled as the Euler–Bernoulli beam. Sheng et al. (2017) studied the dynamic response of the railways under the influence of moving harmonic load by using the Fourier transform method. By using the Green's function method, the dynamic behavior of the railway subjected to accelerated moving load investigated by Ghannadiasl (2017). Thereby, a direct and accurate modeling technique for railway is provided as the Euler-Bernoulli beam on the elastic foundation under the moving load with various boundary conditions. Ghannadiasl et al. (2018) investigated the dynamic analysis of the Euler-Bernoulli cracked beam on the elastic foundation under the concentrated load. Using Green's function natural frequency and deflection of Euler–Bernoulli beam with severel boundary conditions are obtained. Ghannadiasl et al. (2019) also carried out multi-span damped cracked beam by using the desired approach.

The dynamic behavior of the Euler–Bernoulli beam excited by the moving load in the previous studies is assessed. In present work, a precise solution in closed form is illustrated for assessing of soil depth sensitivity to dynamic behavior of the Euler-Bernoulli Beam under accelerated moving load. Also, it might be mentioned here that the previous authors did not provide the effects of time and soil depth for various foundations. The present paper is organized as follows. In section 2, the governing equations based on the Euler-Bernoulli beam theory is illustrated. Then, in section 3, the complete solutions and some numerical examples are provided. In section 4, effects of the soil depth, time and acceleration with some

numerical examples are depicted. Finally, in section 5, the conclusions are classified, briefly.

2. Modelling of the Euler-Bernoulli Beam under Accelerated Moving Load

In present study, an infinite Euler-Bernoulli beam under of different kinds of damping coefficients like beam internal and viscous damping is studied as shown in Fig. 1. The governing differential equation of the Euler-Bernoulli beam is described as below:

$$\left(\frac{\partial^4}{\partial x^4}\left(EI + c_i\frac{\partial}{\partial t}\right) + N\frac{\partial^2}{\partial x^2} + m\frac{\partial^2}{\partial t^2} + c_b\frac{\partial}{\partial t}\right)w(x,t) + P_s = P\delta\left(x - X_F(t)\right) \quad (1)$$

where c_i is the beam internal damping coefficient, N is the axial force, which is assumed positive in compression, m is the beam mass per unit length, P_s is the pressure of foundation that will be switched later, P is the moving load, and v is its velocity. $w(x,t)$ and P show beam displacement and moving load respectively, which are presumed positive when acting downward. Moreover, δ is the Dirac delta function and c_b is the beam viscous damping coefficient.

The equation of the trajectory of the moving load, $X_F(t)$, is illustrated as:

$$X_F(t) = v_{0x}t + \frac{1}{2}a_{0x}t^2 \quad (2)$$

where v_{0x} is the initial speed of the moving load in the x direction, a_{0x} is the constant acceleration of the moving load in the x direction and t refers to time. This function can be described a uniform accelerating motion. On the other hand, the dynamic equilibrium of the soil in the vertical direction illustrated in terms of:

$$\bar{\rho}(v_{0x} + a_{0x}t)^2\frac{\partial^2 u}{\partial s^2} - c_f(v_{0x} + a_{0x}t)\frac{\partial u_r}{\partial s} = \bar{k}_{st}H\frac{\partial^2 u}{\partial z^2} + \bar{G}_s\frac{\partial^2 u}{\partial s^2} \quad (3)$$

where the upper bar illustrates the limitation to the finite strip b, in other words, density and moduli of soil are multiplied by b. u_r is the vertical soil displacement which is used in order to introduce the influence of foundation damping accurately, v is velocity of the load, $\bar{\rho}$ is soil density, $\bar{k}_{st}$ depicts the stiffness, H is soil depth, the expression $\bar{G}_s(\partial^2 y/\partial x^2)$ counts for the shear effect and c_f is the foundation viscous damping coefficient.

All variables will be utilized in dimensionless forms. The critical velocity will be specified by parametric analysis and the systems of Eqs. (1) and (3) will be clarified for steady-state beam deflection. Thereby, changing the equations to moving coordinate $s = x - vt$ and by considering limitation to the steady state conditions gives:

$$\left(EI - c_i(v_{0x} + a_{0x}t)\right)\frac{\partial^4 w}{\partial s^4} + \left(N + m(v_{0x} + a_{0x}t)^2\right)\frac{\partial^2 w}{\partial s^2}$$
$$-(v_{0x} + a_{0x}t)c_b\frac{\partial w}{\partial s} + P_s = P\delta(s) \quad (4)$$

$$\bar{\rho}\left(v_{0x}+a_{0x}t\right)^2\frac{\partial^2 u}{\partial s^2}-c_f\left(v_{0x}+a_{0x}t\right)\frac{\partial u_r}{\partial s}=\bar{k}_{st}H\frac{\partial^2 u}{\partial z^2}+\bar{G}_s\frac{\partial^2 u}{\partial s^2} \quad (5)$$

Initially, the Eq. (4) is solved. Thereafter the relative displacement satisfies the boundary conditions, which makes the determination easier. Thereby

$$z=\zeta H \ , u=u_r+\left(1-\zeta\right)w \quad (6)$$

where z is vertical axis, H is soil depth, u is the beam displacement.

Furthermore with $\chi=\sqrt[4]{\bar{k}_{st}/4EI}$, the moving coordinate s changes to dimensionless coordinate $\xi=\chi s$, and by dividing all terms by the static displacement $w_{st}=p\chi/2\bar{k}_{st}$, to attain dimensionless $\hat{u}_r$ and $\hat{w}$, gives:

$$\left(1-\left(\frac{\vartheta_s}{\alpha}\right)^2\right)\frac{\partial^2\hat{u}_r}{\partial\xi^2}-\frac{\eta_f}{\alpha\mu^2}\frac{\partial\hat{u}_r}{\partial\xi}-\frac{1}{\alpha^2\mu^2}\frac{\partial^2\hat{u}_r}{\partial\zeta^2}=-\left(1-\left(\frac{\vartheta_s}{\alpha}\right)^2\right)\left(1-\zeta\right)\frac{\partial^2\hat{w}}{\partial\xi^2} \quad (7)$$

where, $\vartheta_s=\dfrac{v_s}{v_{cr}}$ shows the shear coefficient which the term v_s in it, stands for the velocity of the shear waves,

$\alpha=\left(v_{0x}+a_{0x}t\right)/v_{cr}$ is the velocity ratio with $v_{cr}=\sqrt[4]{\dfrac{4\bar{k}_{st}EI}{m^2}}$, μ is the mass ratio that explained as $\mu=\sqrt{\bar{\rho}H/m}$, and $\eta_f=\dfrac{c_f H}{\sqrt{\bar{k}_{st}m}}$.

According to the homogeneous conditions, the following relation can be presumed

$$\hat{u}_r=\sum_{j=r}^{\infty}U_j\sin\left(j\pi\zeta\right) \quad (8)$$

Thereafter multiplication with one mode shape, substitution and integration from 0 to 1 depth, and by Fourier transform yields:

$$U_j^*=\frac{\omega^2\dfrac{2}{j\pi}\left(1-\left(\dfrac{\vartheta_s}{\alpha}\right)^2\right)}{-\omega^2\left(1-\left(\dfrac{\vartheta_s}{\alpha}\right)^2\right)-i\omega\dfrac{\eta_f}{\alpha\mu^2}+\left(\dfrac{j\pi}{\alpha\mu}\right)^2}W^* \quad (9)$$
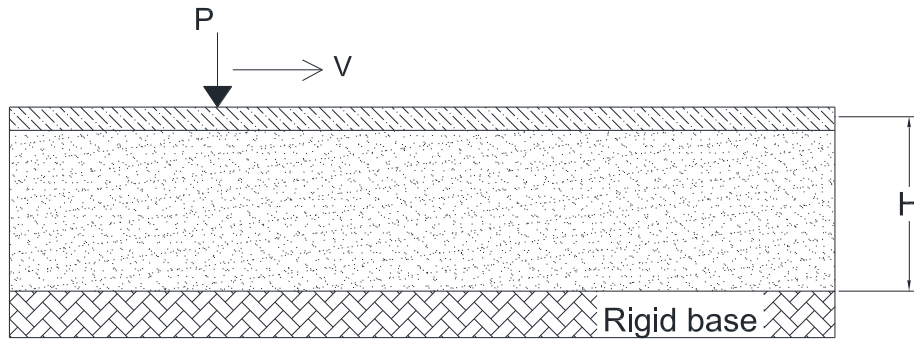

Fig. 1. The infinite beam on soil under accelerated moving load.

According to the foundation pressure as follows (Dimitrovová, 2016):

$$P_s=-\left(1-i\eta_h\right)\bar{k}_{st}\left(\sum_{j=1}^{\infty}j\pi u_j-w\right) \quad (10)$$

where η_h illustrates the coefficient of the hysteretic damping and $u_j=U_j w_{st}$. Hence, getting back to Eq. (1), one attains

$$\left(EI-c_i\left(v_{0x}+a_{0x}t\right)\right)\frac{\partial^4 w}{\partial s^4}+\left(N+m\left(v_{0x}+a_{0x}t\right)^2\right)\frac{\partial^2 w}{\partial s^2}$$
$$-c\left(v_{0x}+a_{0x}t\right)\frac{\partial w}{\partial s}-\left(1-i\eta_h\right)\bar{k}_{st}\left(\sum_{j=1}^{\infty}j\pi u_j-w\right)=P\delta(s) \quad (11)$$

Changes to dimensionless values, here moreover $\eta_i=2\alpha\chi c_i/2\sqrt{mEI}$, $\eta_N=N/2\sqrt{\bar{k}_{st}\left(EI-c_i v\right)}$ and $\eta_b=c_b/2\sqrt{m\bar{k}_{st}}$ are presented.

$$\left(1-\eta_i\right)\frac{\partial^4\hat{w}}{\partial\xi^4}+4\left(\left(\left(\frac{v_{0x}+a_{0x}t}{v_{cr}}\right)^2+\eta_N\right)\frac{\partial^2\hat{w}}{\partial\xi^2}-8\eta_b\frac{\left(v_{0x}+a_{0x}t\right)}{v_{cr}}\frac{\partial\hat{w}}{\partial\xi}\right.$$
$$\left.+4\left(1-i\eta_h\right)\left(\hat{w}-\sum_{j=1}^{\infty}j\pi U_j\right)=8\delta(\xi)\right. \quad (12)$$

By the Fourier transform one acquires:

$$W^*=\frac{8}{\beta+4\left(1-i\eta_b\right)S} \quad (13)$$

and

$$\beta=\left(1-\eta_i\right)\omega^4-4\omega^2\left(\alpha^2+\eta_N\right)-8i\omega\eta_b\alpha+4\left(1-i\eta_h\right)$$

$$S=1+\sum_j\frac{\omega^2\dfrac{2}{j\pi}\left(1-\left(\dfrac{\vartheta_s}{\alpha}\right)^2\right)}{-\omega^2\left(1-\left(\dfrac{\vartheta_s}{\alpha}\right)^2\right)-i\omega\dfrac{\eta_f}{\alpha\mu^2}+\left(\dfrac{j\pi}{\alpha\mu}\right)^2} \quad (14)$$

3. Numerical Examples

An Euler–Bernoulli beam under a moving load is considered for the purpose of verification. The beam is expressed with the following features in Table 1.

Table 1. Numerical data.

Property	Case
Beam bending stiffness EI	$6.4 \left(MN\,m^2 \right)$
Beam mass per unit length m	$60 \left(kg\,/\,m \right)$
Beam damping η_b	0.02
Soil Young's modulus $\bar{E}_s$	$10 \left(MN\,m^{-1} \right)$
Soil Poisson's ratio v	0.2
Soil density $\bar{\rho}$	$185 \left(kg\,/\,m^2 \right)$
Active depth H	$1, 4, 8, 12 \left(m \right)$
Foundation damping η_f	0.629
Force P	$100 \left(kN \right)$
Velocity v_{0x}	$323 \left(m\,/\,s \right)$
Critical velocities v_{cr}^{E-B}	$325 \left(m\,/\,s \right)$

Therefore, by assuming $\eta_i = a_{0x} = 0$, in Eq. (13), the governing equation for the Euler–Bernoulli beam gets as follow (Dimitrovová, 2016):

$$W^* = \frac{8}{\omega^4 - 4\omega^2 \left(\alpha^2 + \eta_N \right) - 8i\omega\eta_b\alpha + 4 \left(1 - i\eta_h \right) S} \tag{15}$$

In order to compare and justify various theoretical models with each other, such as classical Winkler foundation, the model without and with shear contribution, and classical Pasternak and visco-elastic foundations, deflection shapes for these mentioned cases are investigated and shown in Fig 2. By using the presented values, Eq. (13) and by introducing $\vartheta_s = 0$ and $\mu = 0$, solution for classical Winkler's foundation; for $\vartheta_s = 0$ model without shear contribution, for $\mu = 0$ solution for classical Pasternak foundation, and for $\eta_h = 0.529$ model for visco-elastic foundation are attained.

According to the Fig 2, it can be seen that the occupied large area with superior displacement behind the load, stands for the solution without shear contribution. That is because of the vibration of not interacted soil columns. The classical solution for Pasternak, Winkler and visco-elastic foundations provided very low displacement, because the applied velocity is approximately far from the critical one.
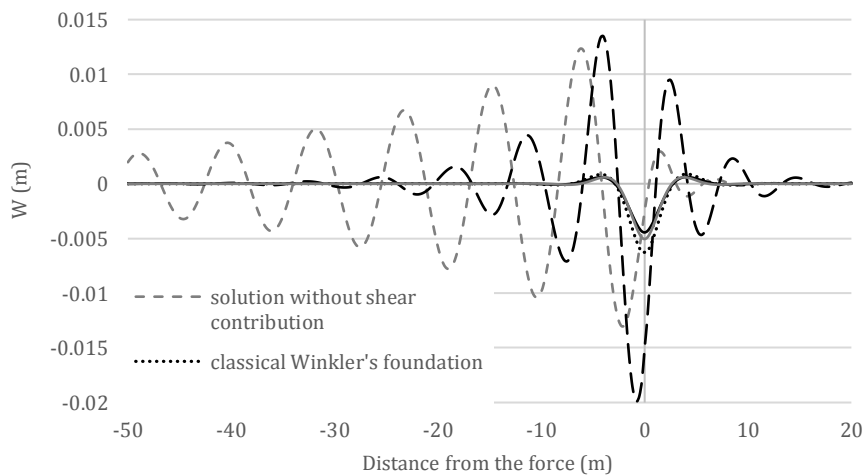

Fig. 2. Deflection shapes comparison for presented values.

On the other hand, the assessment of the critical velocity is shown in Figs. 3 and 4 by deriving the maximum downward and upward displacements. The graphs in Figs 3 and 4 depict that there is rarely any displacement directed upward and downward under the critical velocity. Both of the displacements over the critical velocity, for classical Winkler foundation, the model without and with shear contribution, classical Pasternak foundation, and visco-elastic foundation are compared.

4. Effect of Soil Depth, Time and Acceleration

Analysis of the soil depth and various types of damping are illustrated in this section. The soil depth is surely effective on the dynamic behavior of the beam. So, displacement shapes for different values of active depth ($H = 5, 7, 10, 15m$) are obtained in Figs. 4 and 5. From the figures it is seen that by increasing the soil depth, the displacement of the beam is decreased for both solutions i.e. solution with and without shear contribution. In contrary, the displacement shapes for classical Winkler's foundation, classical Pasternak's foundation and visco-elastic foundation does not changes by increasing of the soil depth because of the value of shear ratio $\mu = 0$.
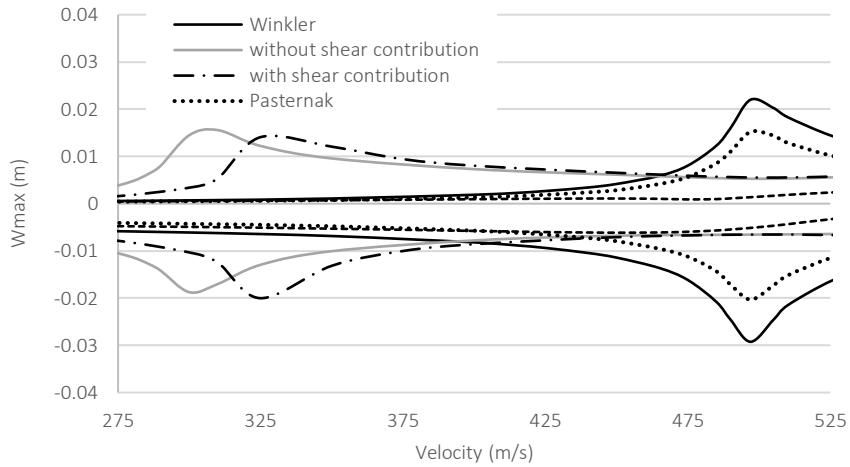
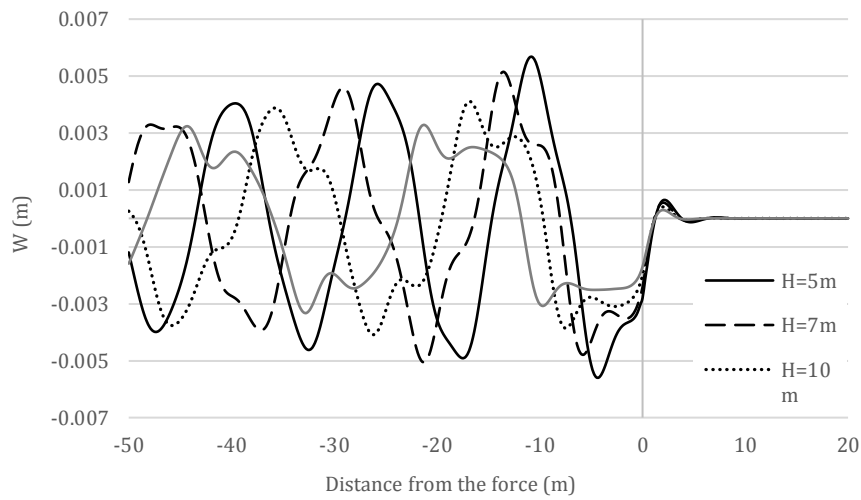**Fig. 3.** Maximum displacements directed downward and upward.

Fig. 4. Displacement shapes for various values of the soil active depth: solution with shear distribution.
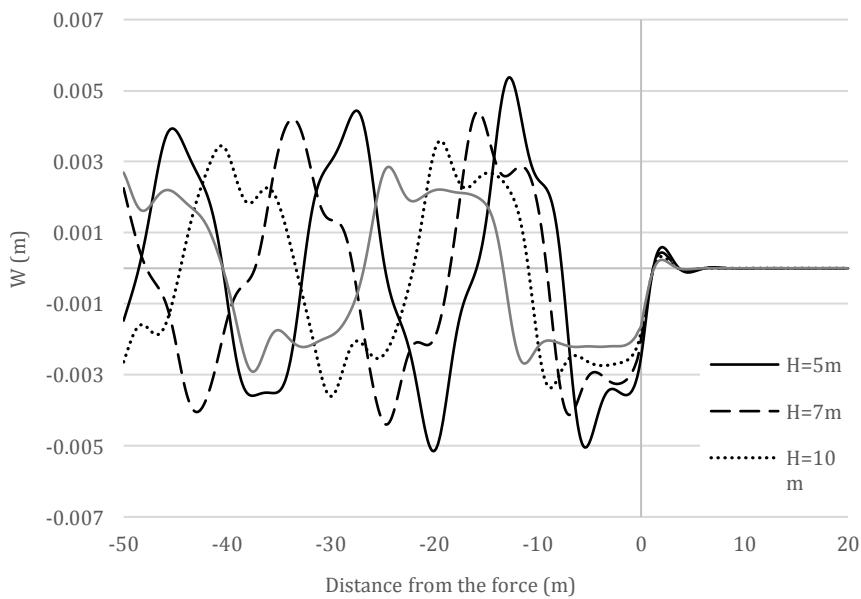

Fig. 5. Displacement shapes for various values of the soil active depth: solution without shear distribution.

As the matter of fact, two factors i.e. acceleration and time play an important role in dynamic behavior of the beam. Therefore, the influence of these two factors on displacement shapes of the beam are provided in Figs. 6 and 7. From Fig. 6 can be seen that by increasing the accelera-

tion of the moving load the displacement of the beam decreases, but when the acceleration soars up to $2000\,\text{m/s}^2$, the displacement of the beam gets stable and approximately reaches zero. Incidentally, according to the Fig. 7, by increasing the time the displacement of the beam decreases.
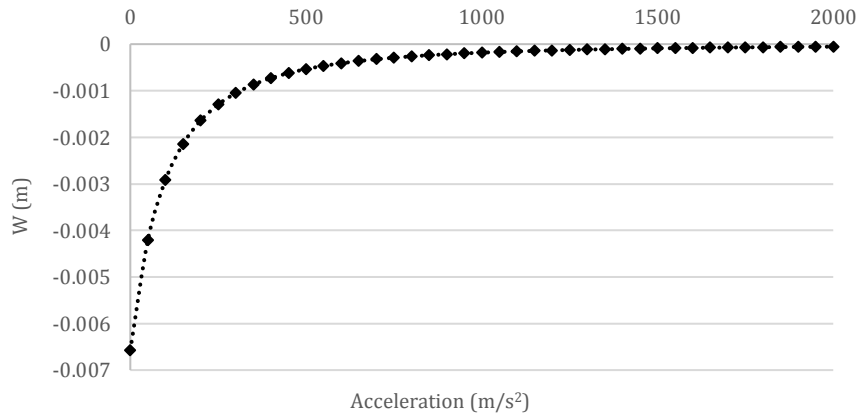

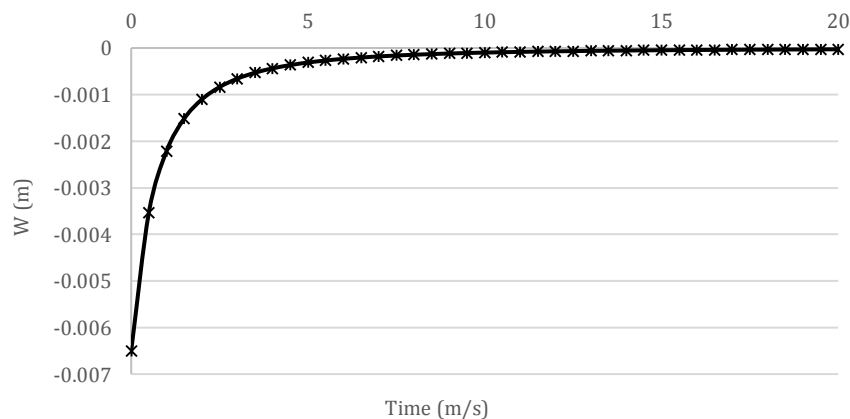**Fig. 6.** Displacement shape for various values of the acceleration on Winkler foundation.

Fig. 7. Displacement shape for various values of the time on Winkler foundation.

5. Conclusions

In this paper, the Euler-Bernoulli beam was analyzed on the various depth of foundation under accelerated moving load and the displacement shapes for different values of active depth were provided. It was shown that the depth of soil is surely effective on the dynamic behavior of the beam. By increasing depth of soil, the displacement of the beam is decreased. On the report of the obtained graphs, it was identified that the occupied large area with superior displacement behind the load stands for the solution without shear contribution. That is because of the vibration does not interacted the soil columns. The classical solution for Pasternak, Winkler and visco-elastic foundations provide very low displacement, because the applied velocity is approximately far from the critical one. It was also declared that, by increasing the acceleration and time zone, the displacement of the beam is decreased. Also, the maximum displacement occurred when the acceleration zone and time are zero.

Publication Note

REFERENCES

Abu-Hilal M (2003). Forced vibration of Euler–Bernoulli beams by means of dynamic Green functions. *Journal of sound and vibration*, 267(2), 191-207.

Balkaya M, Kaya MO, Sağlamer A (2009). Analysis of the vibration of an elastic beam supported on elastic soil using the differential transform method. *Archive of Applied Mechanics*, 79(2), 135-146.

Barari A, Kaliji HD, Ghadimi M, Domairry G (2011). Non-linear vibration of Euler-Bernoulli beams. *Latin American Journal of Solids and Structures*, 8(2), 139-148.

Bazehhour BG, Mousavi SM, Farshidianfar A (2014). Free vibration of high-speed rotating Timoshenko shaft with various boundary conditions: effect of centrifugally induced axial force. *Archive of Applied Mechanics*, 84 (12), 1691-1700.

Bian X, Cheng C, Jiang J, Chen R, Chen Y (2016). Numerical analysis of soil vibrations due to trains moving at critical speed. *Acta Geotechnica*, 11(2), 281-294.

Dimitrovová Z (2016). Critical velocity of a uniformly moving load on a beam supported by a finite depth foundation. *Journal of Sound and Vibration*, 366, 325-342.

Ghannadiasl A (2017). Analytical study of dynamic response of railway on partial elastic foundation under travelling accelerating concentrated load. *International Journal of Transportation Engineering*, 4(4), 317-334.

Ghannadiasl A, Khodapanah Ajirlou S (2018). Dynamic response of multi-cracked beams resting on elastic foundation. *International Journal of Engineering*, 31(11), 1830-1837.

Ghannadiasl A, Khodapanah Ajirlou S (2019). Forced vibration of multi-span cracked Euler–Bernoulli beams using dynamic Green function formulation. *Applied Acoustics*, 148, 484-494.

Gładysz M, Śniady P (2009). Spectral density of the bridge beam response with uncertain parameters under a random train of moving forces. *Archives of Civil and Mechanical Engineering*, 9(3), 31-47.

Györgyi J (1981). Frequency-dependent geometrical stiffness matrix for the vibration analysis of beam systems. *Periodica Polytechnica Civil Engineering*, 25(3-4), 151-163.

Hilal MA, Zibdeh HS (2000). Vibration analysis of beams with general boundary conditions traversed by a moving force. *Journal of Sound and Vibration*, 229(2), 377-388.

Kargarnovin MH, Younesian D (2004). Dynamics of Timoshenko beams on Pasternak foundation under moving load. *Mechanics Research Communications*, 31(6), 713-723.

Kenney JT (1954). Steady-state vibrations of beam on elastic foundation for moving load. *Journal of Applied Mechanics.* 21, 359-364.

Li WL (2000). Free vibrations of beams with general boundary conditions. *Journal of Sound and Vibration*, 237(4), 709-725.

Mehri BA, Davar A, Rahmani O (2009). Dynamic Green function solution of beams under a moving load with different boundary conditions. *Scientia Iranica - Transaction B, Mechanical Engineering*, 273-279.

Mohammadzadeh S, Mosayebi SA (2015). Dynamic analysis of axially beam on visco-elastic foundation with elastic supports under moving load. *International Journal of Transportation Engineering*, 2(4), 289-296.

Motaghian SE, Mofid M, Alanjari P (2011). Exact solution to free vibration of beams partially supported by an elastic foundation. *Scientia Iranica - Transaction A, Civil Engineering*, 18(4), 861.

Prokić A, Bešević M, Lukić D (2014). A numerical method for free vibration analysis of beams. *Latin American Journal of Solids and Structures*, 11(8), 1432-1444.

Sheng X, Zhong T, Li Y (2017). Vibration and sound radiation of slab high-speed railway tracks subject to a moving harmonic load. *Journal of Sound and Vibration*, 395, 160-186.

Timoshenko S (1926). Method of analysis of statical and dynamical stresses in rail. *Proceedings of the Second International Congress for Applied Mechanics, Zurich Switzerland*, 407-418.

Yayli MÖ, Aras M, Aksoy S (2014). An efficient analytical method for vibration analysis of a beam on elastic foundation with elastically restrained ends. *Shock and Vibration*, 2014.

Ying J, Lu CF, Chen WQ (2008). Two-dimensional elasticity solutions for functionally graded beams resting on elastic foundations. *Composite Structures*, 84(3), 209-219.

Zrnić NĐ, Gašić VM, Bošnjak SM (2015). Dynamic responses of a gantry crane system due to a moving body considered as moving oscillator. *Archives of Civil and Mechanical Engineering*, 15(1), 243-250.